International Journal of Nanomedicine

Dovepress
open access to scientific and medical research

Open Access Full Text Article

ORIGINAL RESEARCH

Novel chitosan/agarose/hydroxyapatite nanocomposite scaffold for bone tissue engineering applications: comprehensive evaluation of biocompatibility and osteoinductivity with the use of osteoblasts and mesenchymal stem cells

This article was published in the following Dove Press journal:
International Journal of Nanomedicine

Paulina Kazimierczak[1]
Aleksandra Benko[2]
Marek Nocun[2]
Agata Przekora[1]

[1]Department of Biochemistry and Biotechnology, Medical University of Lublin, Lublin, Poland; [2]Faculty of Materials Science and Ceramics, AGH University of Science and Technology, Krakow, Poland

Background: Nanocomposites produced by reinforcement of polysaccharide matrix with nanoparticles are widely used in engineering of biomaterials. However, clinical applications of developed novel biomaterials are often limited due to their poor biocompatibility.

Purpose: The aim of this work was to comprehensively assess biocompatibility of highly macroporous chitosan/agarose/nanohydroxyapatite bone scaffolds produced by a novel method combining freeze-drying with a foaming agent. Within these studies, blood plasma protein adsorption, osteoblast (MC3T3-E1 Subclone 4 and hFOB 1.19) adhesion and proliferation, and osteogenic differentiation of mesenchymal stem cells derived from bone marrow and adipose tissue were determined. The obtained results were also correlated with materials' surface chemistry and wettability to explain the observed protein and cellular response.

Results: Obtained results clearly showed that the developed nanocomposite scaffolds were characterized by high biocompatibility and osteoconductivity. Importantly, the scaffolds also revealed osteoinductive properties since they have the ability to induce osteogenic differentiation (Runx2 synthesis) in undifferentiated mesenchymal stem cells. The surface of biomaterials is extremely hydrophilic, prone to protein adsorption with the highest affinity toward fibronectin binding, which allows for good osteoblast adhesion, spreading, and proliferation.

Conclusion: Produced by a novel method, macroporous nanocomposite biomaterials have great potential to be used in regenerative medicine for acceleration of the bone healing process.

Keywords: XPS, wettability, protein adsorption, osteogenic differentiation, cell proliferation, cryogel

Introduction

Natural polysaccharides are widely used in engineering of biomaterials and bone tissue engineering (BTE), primarily because of their valuable properties and wide availability. Polysaccharide matrix is often reinforced with nanoparticles to produce nanocomposite scaffolds with improved biodegradability and mechanical properties. Chitosan is one of the most common organic components of bone scaffolds. It is a linear polysaccharide made of deacetylated D-glucosamine units and N-acetyl-D-glucosamine units.[1] The great interest in this polysaccharide is explained by its unique properties, such as high biocompatibility, good host response, bactericidal

Correspondence: Agata Przekora
Department of Biochemistry and Biotechnology, Medical University of Lublin, Chodzki 1 Street, Lublin 20-093, Poland
Tel +48 81 448 7026
Fax +48 81 448 7020
Email agata.przekora@umlub.pl

submit your manuscript | www.dovepress.com
DovePress
http://doi.org/10.2147/IJN.S217245

and bacteriostatic activity, and biodegradability. Moreover, the hydrophilic surface of chitosan and its structure which is similar to bone extracellular matrix (ECM) support osteoblast adhesion, proliferation, and differentiation.[2] Agarose is another natural polymer exhibiting similarity to ECM, which is widely used in BTE. Agarose is a biocompatible and biodegradable natural polysaccharide (made of repeating unit of agarobiose), which has ability to form a gel network allowing diffusion and transport of oxygen and nutrients within the scaffold.[3] Nevertheless, agarose is known to be unfavorable to cell adhesion and it is often combined with other polymers to improve its biocompatibility.[4]

BTE has been developing rapidly for several decades. Nevertheless, clinical applications of engineered constructs are often limited due to poor biocompatibility of developed novel scaffolds. The biocompatibility reflects the ability of biomaterials to exhibit an appropriate systemic and local host response without adverse effects, for instance, cytotoxicity, genotoxicity, and immunogenicity.[5,6] Biocompatible scaffolds for BTE applications should primarily reveal osteoconductive properties by stimulating cell adhesion, proliferation, and formation of bone ECM by the osteoblasts. Osteoconductive scaffolds support bone ingrowth into implanted material and surrounding bone tissue, leading to good osseointegration with the host bone. Ideal biocompatible biomaterials also have osteoinductive properties, which are defined as ability to induce the differentiation of osteoprogenitor cells/stem cells toward osteoblastic lineage.[6,7]

Within this study, biocompatibility of highly macroporous chitosan/agarose/nanohydroxyapatite (chitosan/agarose/nanoHA) bone scaffolds produced by a novel method combining freeze-drying with a gas foaming agent (Polish Patent application number P.426788) was determined. It is worth noting that both the composition of fabricated biomaterials and the method of their production have characteristics of novelty. According to the available literature, there are no papers describing tri-component bone scaffolds made of chitosan-agarose matrix reinforced with nanoHA. Moreover, in BTE, most researchers produce highly macroporous biomaterials by either application of gas foaming agent and freeze-drying method separately or by the use of advanced and expensive techniques, such as 3D printing,[8] electrospinning.[9] The simultaneous application of mentioned (gas foaming and freeze-drying) simple and cost effective methods for the fabrication of the scaffolds allows a highly porous structure with interconnected pores to be obtained, which cannot be obtained by using solely gas foaming agent or freeze-drying method.[4] Investigated here, cryogel nanocomposite scaffolds – containing low or high content of nanoHA – were previously demonstrated to possess bioactivity (ability to form apatite crystals on their surface), high open (70%) and interconnected macroporosity, rough microstructure, non-toxicity, and biodegradability, indicating their promising potential to be used in BTE. Figure 1 shows scanning electron microscopy and microcomputed tomography images of investigated biomaterials. The aim of this work was to comprehensively assess biological response to fabricated novel biomaterials by determination of: 1) human blood plasma protein adsorption to their surfaces, 2) osteoblast adhesion and proliferation (osteoconductive properties), 3) osteogenic differentiation (bone formation) on the surface of the scaffolds and osteoinductive properties with the use of mesenchymal stem cells (MSCs). The obtained results were correlated with materials' surface chemistry and wettability to explain the observed protein and cellular response.

Materials and methods

Preparation of chitosan/agarose/nanoHA scaffolds

Chitosan/agarose/nanoHA scaffolds with low (40 wt%; material marked as chit/aga/HA_L) and high (70 wt%; material marked as chit/aga/HA_H) nanoHA content were synthesized via combining freeze-drying and gas foaming methods, using sodium bicarbonate as a source of CO_2 gas. Briefly, 2 wt% chitosan (75%–85% deacetylation degree, 50–190 kDa molecular weight, viscosity ≤300 cP, Sigma-Aldrich Co., St Louis, MO, USA) and 5 wt% agarose (gel point 36±1.5°C, low EEO, Sigma-Aldrich Co.) were dissolved in 2% acetic acid solution (Avantor Performance Materials, Gliwice, Poland) and mixed with the appropriate quantity of nanoHA and sodium bicarbonate (Sigma-Aldrich Co.). Resultant paste was transferred into cylinder-shaped mold and subjected to heating at 95°C in a water bath, followed by sample cooling, freezing in a liquid nitrogen vapor phase, and freeze-drying (LYO GT2-Basic, SRK Systemtechnik GmbH, Riedstadt, Germany). The final scaffolds were neutralized in 1% NaOH solution (Avantor Performance Materials), washed with deionized water, and air-dried. In the case of X-ray photoelectron spectroscopy (XPS), chitosan/agarose, chitosan, and agarose matrices (without nanoHA) were additionally prepared in an analogous manner to the scaffold production. Before all experiments, the scaffolds were sterilized using ethylene oxide.

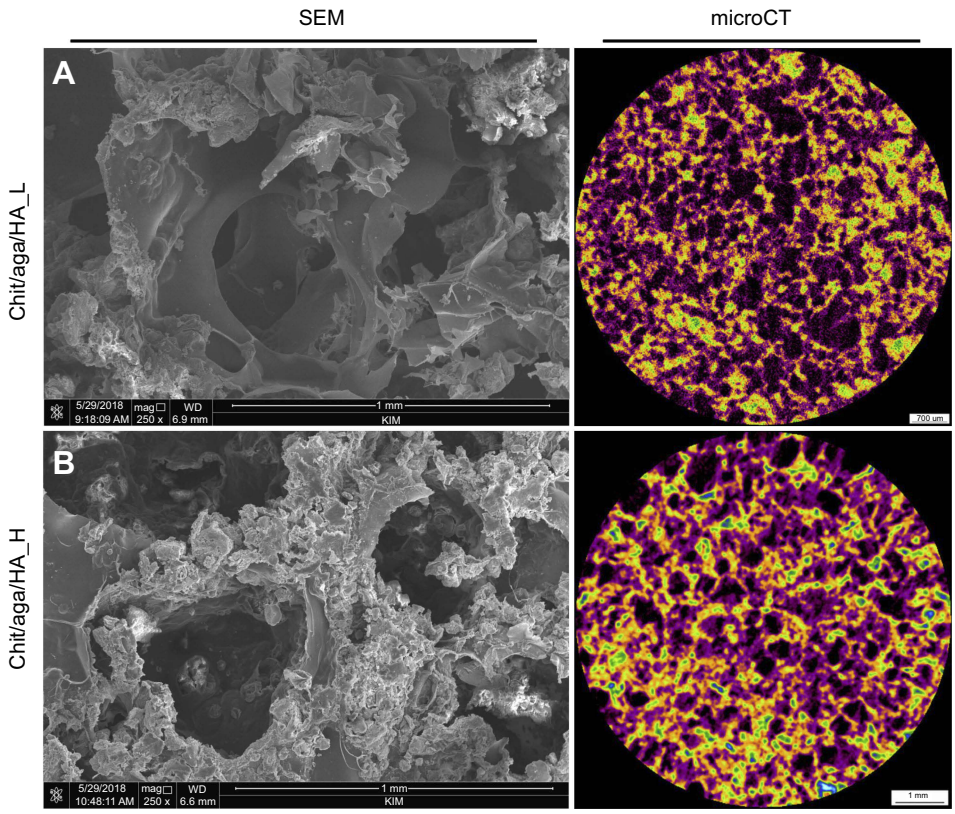

Figure 1 (**A**) Microstructure of the biomaterials visualized by SEM (magnification 250x, scale bar =1 mm). (**B**) MicroCT cross-section images presenting porosity of the scaffolds (black color – pores, yellow/orange/green – nanohydroxyapatite ceramics, violet – polysaccharide matrix).
Abbreviations: SEM, scanning electron microscopy; microCT, microcomputedtomography; chit/aga/HA_L, chitosan/agarose/nanohydroxyapatite scaffolds with low [40 wt%] nanohydroxyapatite content; chit/aga/HA_H, chitosan/agarose/nanohydroxyapatite scaffolds with high [70 wt%] nanohydroxyapatite content.

Evaluation of surface chemical properties

XPS (Vacuum Systems Workshop Ltd., England) was applied to reveal the composition of chemical species present at the surface of material. In this system, the spatial resolution is approximately 3 mm and the signal is recorded from approximately 5 nm deep, so a single measurement is assumed to be representative of the surface chemistry of each material. Mg Ka X-ray radiation with 200 W was used as an excitation source and the electron energy analyzer was set to FAT mode with pass energy equal to 22 eV. After the measurement, the spectra were calibrated assuming the binding energy of C1s to always be equal to 284.6 eV. Quantitative evaluation was done on XPS Peak 4.1 software by deconvoluting the peaks using their areas.

Wettability test

Wettability of the materials was evaluated by the static contact angle method using DSA 25 (Kruss GmbH, Hamburg, Germany) goniometer. Ultra pure water (Polwater DL-100 deionizer, Labopol-Polwater, Krakow, Poland) was used in the study. For each type of material, at least three separate samples were evaluated and each of those were tested at least in triplicate to establish repeatability of the observed wetting behavior.

Protein adsorption tests

Quantitative estimation of protein adsorption

Protein adsorption test was carried out in accordance with the procedure described previously.[10] In brief, wetted disc-shaped scaffolds, approximately 2 mm thick and 5 mm in diameter, were placed in a 96-multi-well plate and incubated for 3 hours at 37°C on a shaker (125 rpm, Sky Line DTS-4, ELMI Ltd., Riga, Latvia) in human blood plasma (collected from a healthy volunteer after obtaining written informed consent) or in human protein solutions (1 mg/mL) prepared in PBS (Pan-Biotech GmbH, Aidenbach, Bavaria, Germany): albumin, fibrinogen (Sigma-Aldrich Co.), fibronectin (BD Biosciences, San Jose, CA, USA). Empty wells of polystyrene (PS) 96-multi-well plate with protein

solutions were treated as a test control to check unspecific binding of proteins to PS. After 3 hours' incubation, protein solutions were discarded, scaffolds were moved into new wells of 96-multi-well plate, washed four times with PBS, and incubated in 1% sodium dodecyl sulfate solution (Sigma-Aldrich Co.) for 1 hour on the shaker (230 rpm) to recover proteins adsorbed to the samples. Protein concentrations in the collected solutions were assessed using the Lowry method as described previously.[10] Results were expressed as the quantity of adsorbed proteins (μg) per 1 cm^2 of the scaffold.

Qualitative estimation of protein adsorption

Scaffolds were incubated in human blood plasma and protein solutions as described in the section "Quantitative estimation of protein adsorption". After the washing step, proteins adsorbed to the surface of the samples were fixed with 3.7% paraformaldehyde (Sigma-Aldrich Co.) for 10 minutes and visualized by immunofluorescence (IF) technique using human-specific anti-albumin, anti-fibrinogen, and anti-fibronectin primary antibodies (Abcam, Cambridge, England). Scaffolds were incubated overnight at 4°C with primary antibodies prepared at a concentration in the range 1–5 μg/mL, washed five times with PBS, and subsequently incubated for 1 hour at room temperature with secondary antibodies conjugated to AlexaFluor®405, AlexaFluor®488, or AlexaFluor®647 (Abcam), prepared at a concentration of 2 μg/mL. Untreated scaffolds incubated with primary and secondary antibodies served as test control to check unspecific binding of antibodies to the scaffolds. Proteins adsorbed to the scaffolds were observed using a confocal laser scanning microscope (CLSM, Olympus Fluoview equipped with FV1000, Olympus, Corporation, Tokyo, Japan).

Cell culture experiments

The cell culture experiments were conducted using disc-shaped scaffolds approximately 3 mm thick and 8 mm in diameter. Prior to the cell culture experiments, samples were placed in the wells of 48-multi-well plate and pre-incubated overnight in an appropriate complete culture medium at 37°C. Cell adhesion and proliferation tests were performed using osteoblast cell lines: normal mouse calvarial preosteoblast cell line (MC3T3-E1 Subclone 4, ATCC-LGC Standards, Teddington, UK) and normal human fetal osteoblast cell line (hFOB 1.19, ATCC-LGC Standards) which were cultured as described previously.[11]

Evaluation of osteogenic differentiation and osteoinductive properties of the scaffolds was carried out using human bone marrow-derived mesenchymal stem cells (BMDSCs) (ATCC-LGC Standards) and adipose tissue-derived mesenchymal stem cells (ADSCs) isolated from adipose tissue of a female dog (fat tissue was collected during sterilization procedure after obtaining written informed consent from the dog owner). BMDSCs were cultured at 37°C in a humidified atmosphere containing 5% CO_2, in Mesenchymal Stem Cell Basal Medium (ATCC-LGC Standards) supplemented with 10 U/mL penicillin, 10 μg/mL streptomycin (Sigma-Aldrich Co.), and the components of Bone Marrow-Mesenchymal Stem Cell Growth Kit (ATCC-LGC Standards). ADSCs were cultured at 37°C in a humidified atmosphere containing 5% CO_2, in a 1:1 mixture of DMEM/Ham's F12 medium without phenol red, supplemented with 2.5 mM L-glutamine (Sigma-Aldrich Co.), 10% FBS, 10 ng/mL rhFGF, 5 ng/mL rhEGF (Pan-Biotech GmbH, Aidenbach, Bavaria, Germany), 100 U/mL penicillin, and 100 μg/mL streptomycin. ADSCs were isolated from the dog adipose tissue according to the procedure described elsewhere.[12] Briefly, fat tissue was cut with surgical scissors into small pieces, washed several times with PBS, and digested with 0.1% collagenase solution (Gibco, Thermo Fisher Scientific, Waltham, MA, USA) for 1 hour at 37°C on a shaker. Obtained fat solution was then subjected to four centrifuge steps (4 minutes at 21°C, 300×*g*), the pellet (stromal vascular fraction) was resuspended in the culture medium, filtered using a cell strainer (BD Falcon, Sigma-Aldrich Co.), and plated into T75 culture flasks (Figure 2A). IF staining of specific ADSC markers was carried out to confirm successful isolation of dog ADSCs (Figure 2B). Briefly, the isolated cells were seeded in the wells of 48-multi-well plate, fixed with 3.7% paraformaldehyde, permeabilized with 0.2% Triton X-100 (Sigma-Aldrich Co.), blocked with 1% bovine serum albumin (Sigma-Aldrich Co.), and then incubated overnight at 4°C with dog-specific anti-integrin β1/CD29 and anti-CD90/Thy1 primary antibodies (R&D Systems, Inc., Minneapolis, MN, USA), prepared at a concentration of 10 μg/mL. Then, the cells were washed with PBS and incubated for 1 hour at room temperature with secondary antibodies conjugated to AlexaFluor®647 (Abcam) or NL493 (R&D Systems Inc.), prepared at a concentration of 2 μg/mL. Stained cells were observed under CLSM using two-dimensional laser scanning technique.

Cell adhesion, spreading, and proliferation

MC3T3-E1 cells and hFOB 1.19 osteoblasts were seeded directly on the scaffolds in 500 μL of complete culture medium at a density of 5×10^4 cells/mL. Cells cultured in

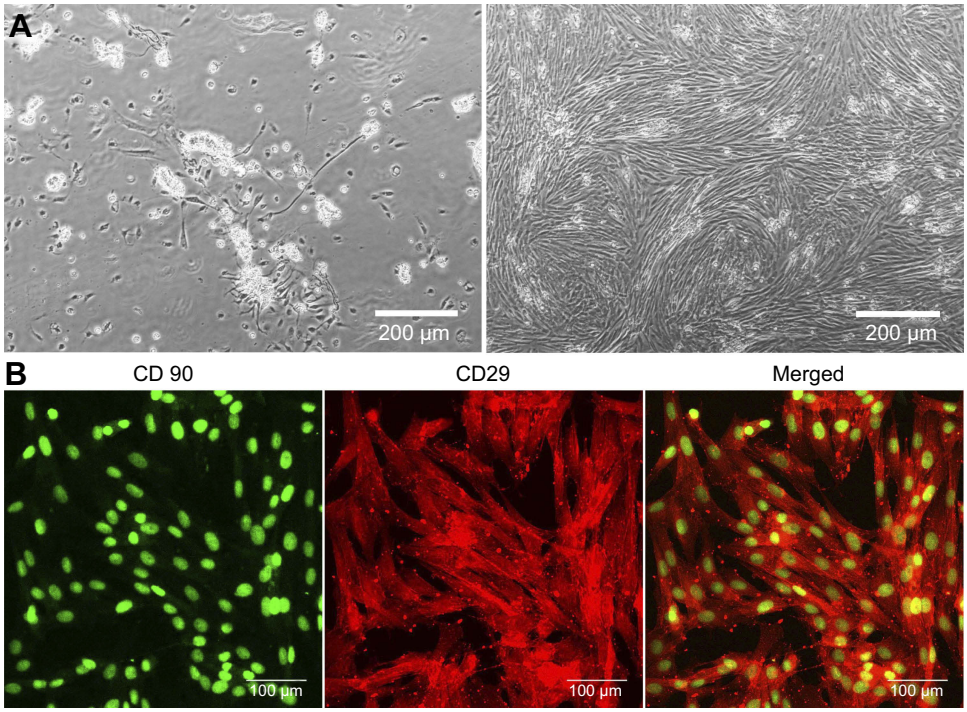

Figure 2 (**A**) Phase-contrast images presenting growth of isolated ADSCs 24 hours (on the left) and 4 days (on the right) after plating the SVF onto T75 culture flask (magnification 100x, scale bar =200 µm); (**B**) CLSM images showing immunofluorescent staining of markers typical of ADSCs (CD90 – green fluorescence, CD29 – red fluorescence; magnification 400x, scale bar =100 µm).
Abbreviations: ADSCs, adipose tissue-derived mesenchymal stem cells; SVF, stromal vascular fraction; CLSM, confocal laser scanning microscope.

the PS well of 48-multi-well plate served as a control. On the 2nd (cell adhesion and spreading test) as well as on the 3rd, 6th, and 9th day (proliferation test), the cells were fixed as described in the previous section. Then, the samples were incubated for 30 minutes at room temperature with the solution containing two units of AlexaFluor635-conjugated phallotoxin (Thermo Fisher Scientific) and 0.5 µg/mL DAPI (Sigma-Aldrich Co.) to label cytoskeleton filaments (F-actin) and nuclei, respectively. Stained cells were examined under CLSM. Spreading area of at least 50 individual cells grown on three different scaffold samples (n=3) were measured using ImageJ software. The number of cells on the surface of the scaffold at each time interval was estimated via counting of cell nuclei (ImageJ software).

Osteogenic differentiation and osteoinductive properties

BMDSCs and ADSCs (at passage 2) were seeded directly on the samples in 500 µL of complete culture medium at a density of 2×10^5 cells/mL. After 24-hour culture at 37°C, the complete culture medium was replaced with osteogenic medium consisting of complete culture medium supplemented with 0.05 mg/mL ascorbic acid, 10 mM β-glycerophosphate, and 10^{-8} M dexamethasone (dex) (all reagents purchased from Sigma-Aldrich Co.). In order to assess osteoinductive properties of the scaffolds, a parallel experiment with the use of osteogenic medium without dex was performed. The experiment was carried out for 21 days, and half of the culture medium was replaced with a fresh portion every 3rd day. On the 3rd, 7th, and 21st day of the experiment, markers of the osteogenic differentiation were quantified in the cell lysates using appropriate ELISA kits specific to human and dog species: type I collagen (Col I, EIAab ELISA kit, Wuhan, China), bone alkaline phosphatase (bALP, FineTest ELISA kit, Wuhan, China), and osteocalcin (OC, EIAab ELISA kit, Wuhan, China). The cell lysates were prepared in accordance with the procedure described previously by repeated freeze-thaw cycles followed by ultrasonication.[11] Additionally, IF staining of Col I (on the 3rd and 7th day) and Runx2 (on the 7th day) was performed. The samples were fixed and permeabilized as described before, and then incubated overnight at 4°C with primary antibodies prepared at a concentration of 10 µg/mL: human/dog specific anti-Runx2 (Abcam), human-specific anti-collagen I (Col1a1/Col1a2) (Abnova, Taoyuan City, Taiwan), and dog-specific collagen I and III (Abcam). Then, the samples were washed with PBS and incubated for 1 hour at room temperature with secondary antibodies

conjugated to Alexa-Fluor®488, AlexaFluor®532, or AlexaFluor®647 (Abcam), prepared at a concentration of 2 µg/mL. Additional counter-staining with 0.5 µg/mL DAPI was applied for samples stained with primary anti-collagen antibodies. Stained cells were observed using a CLSM.

Statistical analysis

All experiments (except for XPS) were carried out at least in triplicate (n=3). Statistically significant results between samples were considered at $P<0.05$ and were determined using unpaired *t*-test or one-way ANOVA followed by Tukey's test (GraphPad Prism 8.0.0 Software). The data were presented as mean values ± SD.

Results and discussion

Evaluation of surface chemical properties

XPS evaluation revealed different surface chemistry of the tested nanocomposite materials (Figure 3A). In chit/aga/HA_H, the overall amount of oxygen and nitrogen atoms was approximately 56.8 and 1.7%, respectively, while in the case of chit/aga/HA_L, their amount was 41.5 and 1.4%, respectively. Higher amount of oxygen in chit/aga/HA_H was most likely a direct consequence of the presence of higher amount of HA in this material (XPS evaluation of HA indicated oxygen content close to 58%, Figure 3B). Both materials were also found to have an increased amount of nitrogen, when compared to pure chit/aga, with higher values observed for chit/aga/HA_H (1.7% compared to 1.4%), which might suggest presence of chemical interactions between the polysaccharide matrix and HA (Figures 3 and 4). Deconvolution revealed that in both materials the majority of carbon atoms was in the polymer backbone and the rest existed in various oxygen and nitrogen connected functional groups. Evaluation of oxygen species revealed that in chit/aga/HA_L (Figure 3A) there was a high share of hydroxyl groups (similar to pure polymers, Figure 4A), with a small share of O-C-O and O-C=O species, while for chit/aga/HA_H, most of the atoms were in the C=O and amide bonds and only a few in OH (Figure 3A). Nitrogen peak evaluation revealed that in the chit/aga/HA_L (Figure 3A), all of the nitrogen atoms were in protonated amide/amine species (like in chitosan, Figure 4A), while in the chit/aga/HA_H, in various types of =N- bonds (Figure 3A).[13,14] All of the obtained results indicated that there were chemical interactions between the polymers and HA, causing changes in the chemical composition of the surface of the materials. These interactions were found to be more significant for the higher shares of HA. Functional groups in chit/aga/HA_L were more polar, which according to the literature, should generally result in lower strength of plasma protein adsorption.[15]

Wettability test

Wettability of the material is an important parameter dictating the rate of adhesion and conformation of proteins to the surface of material, which, in turn, impact the cell behavior.[15] In this study, static contact angle measurements were applied to evaluate the wetting characteristic of the materials. However, it was soon found that obtaining reliable measurements was impossible, due to high absorbency of the materials, resulting in complete wetting and spontaneous disappearance of the water droplet from the surface of material (movie clips representing this phenomenon on both types of material can be seen in Supplementary Videos S1 and S2). It can be seen that on the chit/aga/HA_H surface (SD2), the water droplet disappeared slightly slower than on the chit/aga/HA_L (SD1), which – as revealed by XPS – was more polar and charged, attracting water more strongly. All of these observations suggested that surface of chit/aga/HA_H material was slightly less hydrophilic, which should in turn result in increased plasma protein adsorption.[15]

Protein adsorption tests

Just after implantation of bone scaffolds into a living organism or after contact of the biomaterials with FBS-containing cell culture medium, their surfaces are instantly coated with the plasma/serum proteins.[16] In this study, we investigated the ability of the developed scaffolds to adsorb albumin, fibrinogen, and fibronectin due to their specific roles in the bone formation process and biocompatibility of the biomaterials. Albumin is the most abundant protein in human blood, which has the ability to easily adsorb to various surfaces. This protein was demonstrated to prevent adhesion of inflammatory cells like neutrophils or macrophages, protecting against biomaterial-induced inflammatory response.[17] Fibronectin is a glycoprotein (belonging to the cell adhesive proteins) that is involved in the interactions with cell membrane integrins, which is a critical step for strong adhesion and subsequent survival and growth of anchorage-dependent cells.[16] Whereas adsorption of fibrinogen to the biomaterials was proven to promote macrophage adhesion followed by their transition toward anti-inflammatory phenotype (M2),

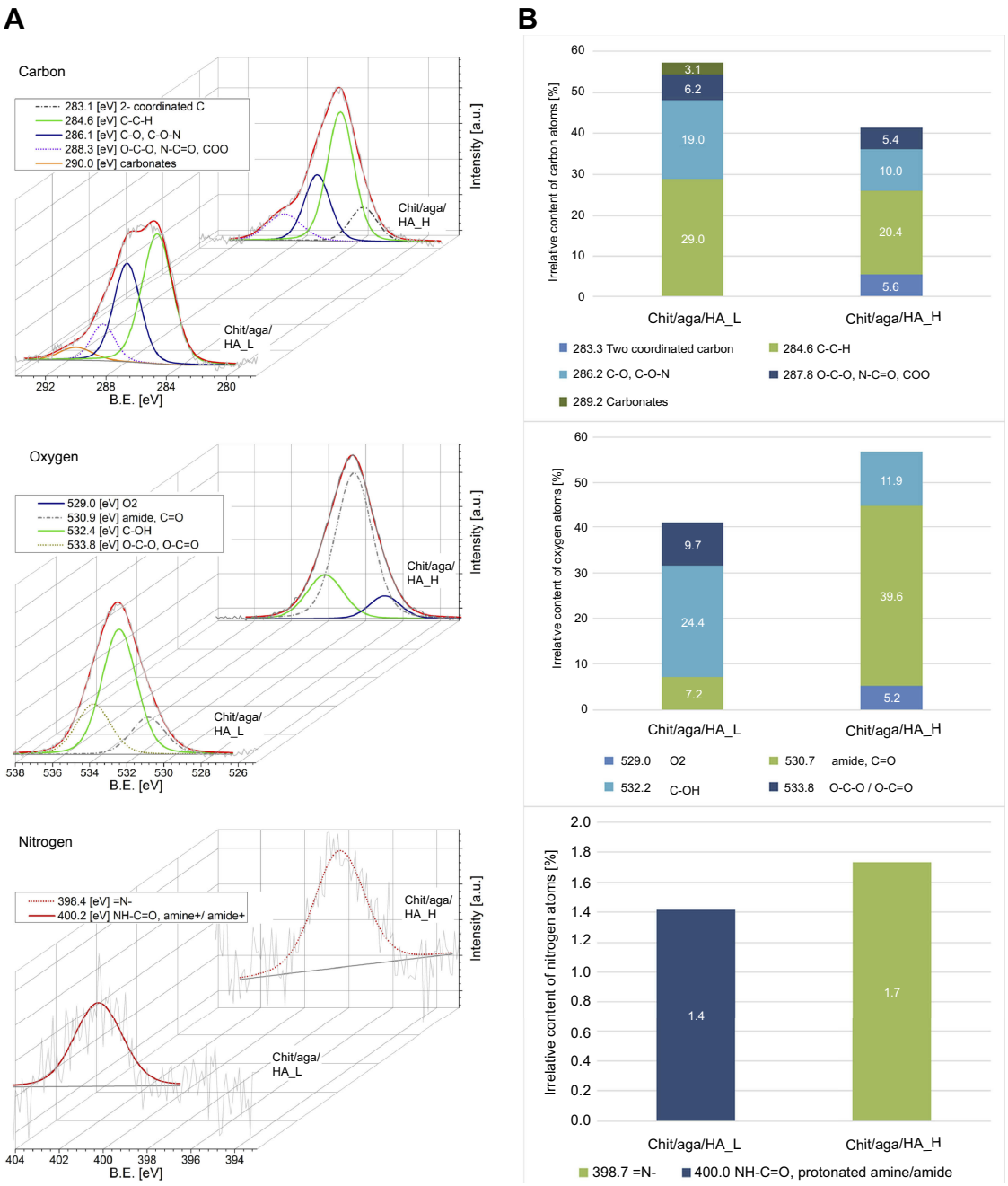

Figure 3 (**A**) Deconvoluted XPS peaks, revealing chemical states of atoms and allowing for identification of functional groups present on the surface of the scaffolds. (**B**) Quantitative evaluation of the chemical species, based on the peaks' areas.

Abbreviations: XPS, X-ray photoelectron spectroscopy; chit/aga/HA_L, chitosan/agarose/nanohydroxyapatite scaffolds with low [40 wt%] nanohydroxyapatite content; chit/aga/HA_H, chitosan/agarose/nanohydroxyapatite scaffolds with high [70 wt%] nanohydroxyapatite content.

which is known to enhance bone regeneration and angiogenesis at the implantation area.[18,19]

As shown in Table 1, the chit/aga/HA_H adsorbed meaningfully more proteins compared to the chit/aga/HA_L, however statistically significant results were obtained only for plasma proteins and fibronectin. Moreover, comparison of protein adsorption from various protein solutions applied at the same concentration of 1 mg/mL, showed that both scaffolds exhibited the highest affinity toward adsorption of fibronectin and the lowest toward albumin. In general, it is known that proteins adsorb better to hydrophobic surfaces, except for glycoproteins (eg, fibronectin, vitronectin, laminin – main cell adhesive proteins) which show higher affinity to polar and

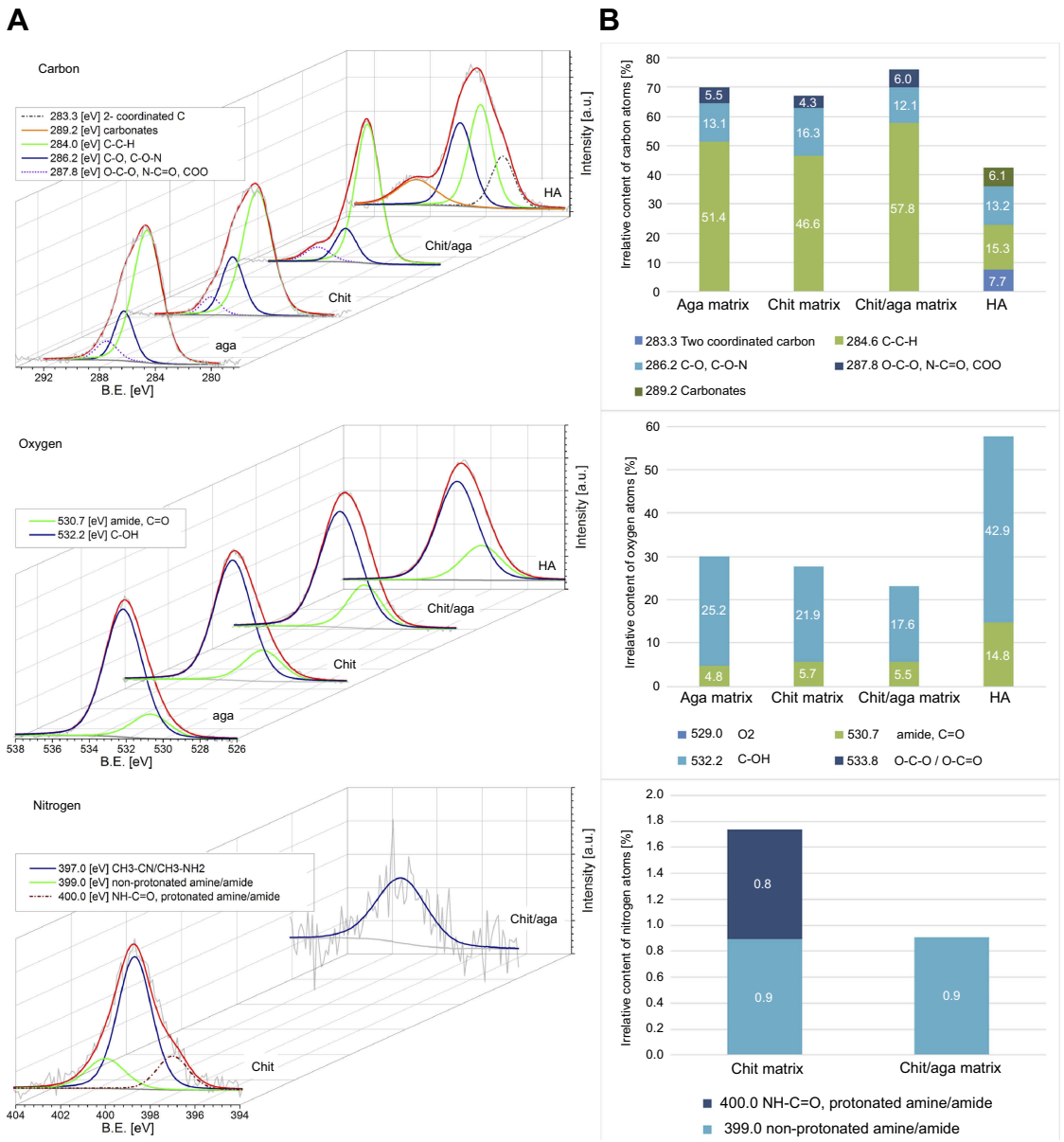

Figure 4 (**A**) Deconvoluted XPS peaks, revealing chemical states of atoms and allowing for identification of functional groups present on the surface of individual components of the materials (chitosan, agarose, chitosan/agarose matrix, and nanoHA). (**B**) Quantitative evaluation of the chemical species, based on the peaks' areas.
Abbreviations: XPS, X-ray photoelectron spectroscopy; aga, agarose; chit, chitosan; HA, hydroxyapatite.

Table 1 Amount of adsorbed proteins to the chit/aga/HA_L and chit/aga/HA_H from human blood plasma and 1 mg/mL protein solutions

Amount of adsorbed proteins [μg/cm^2]				
	Human blood plasma	**Albumin solution**	**Fibrinogen solution**	**Fibronectin solution**
chit/aga/HA_L	647.80±64.54	15.21±5.06	32.71±6.57	69.14±1.84
chit/aga/HA_H	763.20±86.00*	20.82±2.60	41.28±3.49	83.83±1.84*

Notes: *Statistically significant results compared to the chit/aga/HA_L (n=3, $P<0.05$, unpaired *t*-test).
Abbreviations: chit/aga/HA_L, chitosan/agarose/nanohydroxyapatite scaffolds with low [40 wt%] nanohydroxyapatite content; chit/aga/HA_H, chitosan/agarose/nanohydroxyapatite scaffolds with high [70 wt%] nanohydroxyapatite content.

hydrophilic surfaces due to the presence of hydrophilic glycans which hide the hydrophobic domains of the proteins inside a hydrophilic shell.[15,20] Interestingly, some functional groups (eg, OH, COOH, CH_3, NH_2) present on the surface of the material may also affect fibronectin binding.[21,22] Both developed scaffolds showed highly

hydrophilic surfaces (complete wetting, movie clips SD1 and SD2) which resulted in the highest affinity toward fibronectin (glycoprotein) binding. Nevertheless, chit/aga/HA_L had higher share of hydroxyl groups on the surface (Figure 3A) which slightly reduced its ability to adsorb fibronectin compared to the chit/aga/HA_H (Table 1). This observation is in good agreement with Lee et al's findings that demonstrated the lowest fibronectin adsorption to the surface with OH functional groups.[22] Furthermore, the slightly less hydrophilic surface of the chit/aga/HA_H resulted in higher protein adsorption ability of this scaffold compared to chit/aga/HA_L.

Immunofluorescent staining showed a great number of adsorbed proteins on the surface of the scaffolds (Figure 5A and B). Moreover, double staining of albumin + fibrinogen and albumin + fibronectin after scaffold incubation in human blood plasma confirmed the highest affinity of biomaterials toward fibronectin binding (Figure 5B). Interestingly, CLSM images obtained after incubation of biomaterials in human blood plasma showed that scaffolds with lower content of nanoHA – unlike chit/aga/HA_H – induced conversion of fibrinogen to fibrin fibrils. This might be a result of strong polar interactions between the proteins and polar groups on the surface of chit/aga/HA_L, which might have induced conformation changes in the adhered proteins, changing their functionality. Fibrinogen has the ability to bind growth factors like FGF-2 and VEGF, and thus to promote angiogenesis.[23] Therefore, conversion of fibrinogen to fibrin fibrils may potentially worsen its affinity toward growth factors, reducing chit/aga/HA_L scaffold's biocompatibility. Nevertheless, both fabricated biomaterials not only had the ability to adsorb a large amount of plasma proteins, but also exhibited high affinity to fibronectin (cell adhesive protein) and fibrinogen (responsible for enhancement of bone formation and angiogenesis), which has the greatest biomedical importance.

Cell adhesion and spreading

According to available literature, hydrophilic, rough, and polar surfaces of biomaterials are known to promote adsorption of

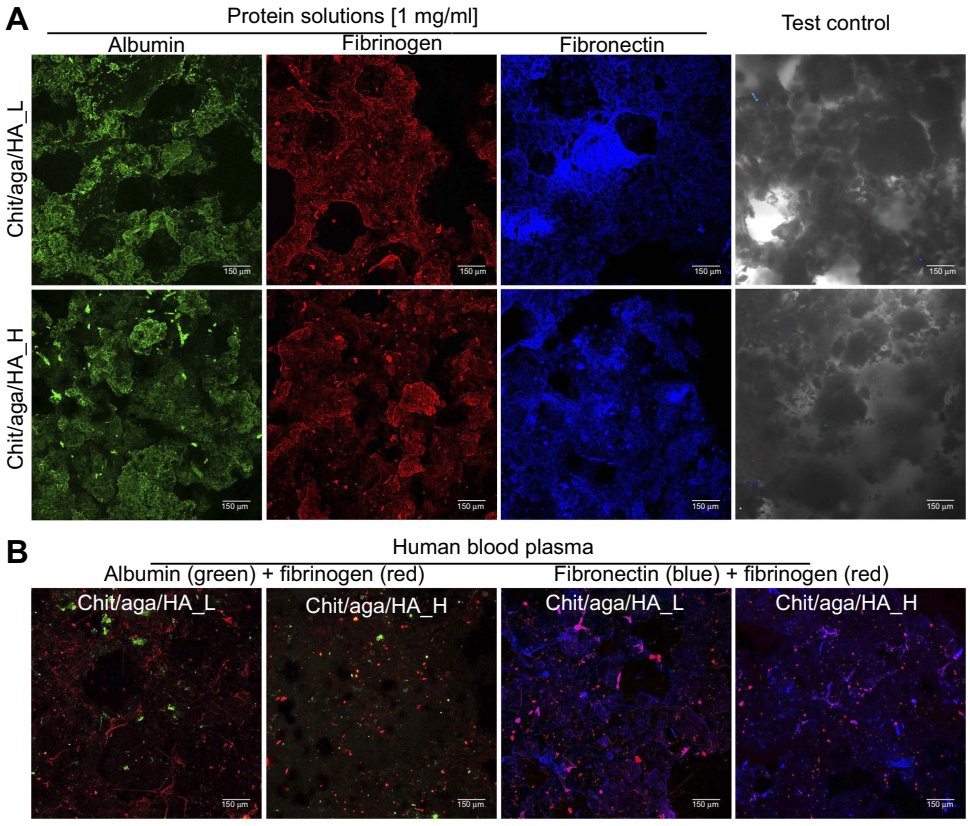

Figure 5 CLSM images presenting immunofluorescent staining of adsorbed proteins to the surface of the chit/aga/HA_L and chit/aga/HA_H scaffolds. (**A**) Experiment with the use of protein solutions at concentration of 1 mg/mL, (**B**) experiment with the use of human blood plasma (albumin – green fluorescence, fibrinogen – red fluorescence, fibronectin – blue fluorescence; Nomarski contrast was applied for the test control to visualize scaffolds' structure; magnification 100x, scale bar =150 μm).

Abbreviations: CLSM, confocal laser scanning microscope; chit/aga/HA_L, chitosan/agarose/nanohydroxyapatite scaffolds with low [40 wt%] nanohydroxyapatite content; chit/aga/HA_H, chitosan/agarose/nanohydroxyapatite scaffolds with high [70 wt%] nanohydroxyapatite content.

cell adhesive proteins (laminin, fibronectin, vitronectin) and to provide the best adhesion and spreading of osteoblasts/stem cells.[16,24,25] Both scaffolds showed extremely hydrophilic surfaces, which were proven to have the highest affinity for fibronectin binding (Table 1), suggesting their positive impact on cell adhesion and spreading. Performed IF staining of F-actin filaments confirmed that both developed biomaterials supported strong cell adhesion since MC3T3-E1 and hFOB 1.19 osteoblasts cultured on their surfaces were well spread and formed a visible junction between actin cytoskeleton and the scaffold (Figure 6A). Although chit/aga/HA_H adsorbed significantly more fibronectin compared to chit/aga/HA_L, measurements of cell spreading area did not reveal statistical differences between the scaffolds (Figure 6B). Control cells grown in the PS well showed significantly higher spreading area compared to the osteoblasts cultured on the scaffolds. It is a normal phenomenon since cells grown on 3D biomaterials and also those occurring in a living organism exhibit different morphology and more spatial growth compared to osteoblasts grown on a 2D culture model.

Cell proliferation evaluation

Biocompatible bone scaffolds should not only support strong cell adhesion to the surface of biomaterials, but also promote cell proliferation to ensure sufficient cell biomass for osteogenic differentiation and bone formation process.[11] The number of cells on the surface of biomaterials was examined 3, 6, and 9 days after seeding. Figure 7 shows that both developed scaffolds supported proliferation of MC3T3-E1 and hFOB 1.19 osteoblasts, which were well spread, formed extensive cytoskeleton structure, and almost reached confluence on the 9th day of the experiment. MC3T3-E1 cells showed similar proliferation on both fabricated biomaterials (statistically significant differences were observed only for 6th day). On the 9th day of the experiment, the number of MC3T3-E1 cells on the surface of chit/aga/HA_L and chit/aga/HA_H was equal to $(6.75\pm2.14)\times10^4$ cells per cm^2 and $(5.56\pm0.15)\times10^4$ cells per cm^2, respectively (Figure 7A).

Nevertheless, significant differences between number of hFOB 1.19 cells on the chit/aga/HA_L and chit/aga/HA_H biomaterial were observed (Figure 7B). The scaffold with higher content of nanoHA, which also adsorbed significantly more fibronectin, was significantly more favorable to human osteoblast proliferation compared to the chit/aga/HA_L. On the 3rd day of the experiment, the amount of hFOB 1.19 cells on the surface of chit/aga/HA_L was almost 2-fold lower than on the chit/aga/HA_H. Whereas, after the 9th day of culture, the amount of hFOB 1.19 cells on the surface of chit/aga/HA_L and chit/aga/HA_H was equal to $(7.80\pm1.93)\times10^4$ cells per cm^2 and $(10.12\pm2.09)\times10^4$ cells per cm^2, respectively.

Control cells grown in the PS multi-well plate proliferated significantly faster than cells cultured on the scaffold surfaces (Figure 7A and B) what resulted from optimal growth substrate for osteoblasts (tissue culture-treated PS). Moreover, it is commonly observed that cells grown on 3D scaffolds need more time for adaptation (Lag phase) to the culture conditions which leads to a delay in

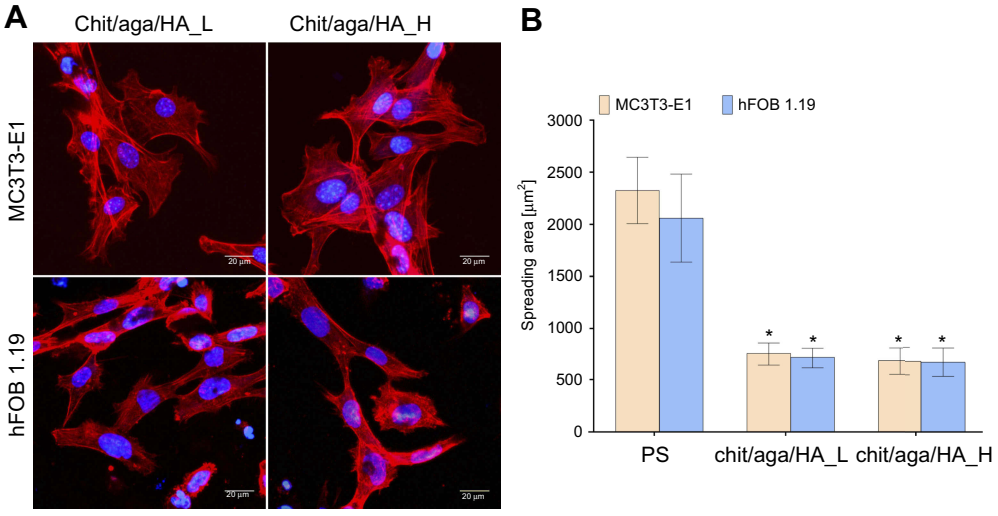

Figure 6 Evaluation of cell adhesion and spreading on the surface of the scaffolds after 48-hour cell culture. (**A**) Fluorescent staining of cell cytoskeleton (F-actin – red fluorescence, nuclei – blue fluorescence; 40x objective and zoom factor 2, scale bar =20 µm). (**B**) Quantitative analysis of spreading area (polystyrene [PS] – control cells grown in PS well).
Abbreviations: chit/aga/HA_L, chitosan/agarose/nanohydroxyapatite scaffolds with low [40 wt%] nanohydroxyapatite content; chit/aga/HA_H, chitosan/agarose/nanohydroxyapatite scaffolds with high [70 wt%] nanohydroxyapatite content.

the start of logarithmic (Log) growth phase compared to the cells grown on a 2D culture model on flat substrate growth (like cell culture dishes). Nevertheless, on the 9th day of the experiment the number of human hFOB 1.19 osteoblasts on the surface of chit/aga/HA_H (10.12×10^4 cells per cm^2) was comparable to the number of cells in PS well (12.16×10^4 cells per cm^2) (Figure 7B).

Osteogenic differentiation

MSCs derived from bone marrow (BMDSCs) or adipose tissue (ADSCs) are promising cells for extensive applications in BTE. Osteogenic differentiation of MSCs can be divided into three stages which are distinguished by the expression of specific markers: 1) proliferation (Runx2, Col I, fibronectin, low bALP activity), 2) ECM synthesis (high bALP activity, Col I, Runx2, Osterix), and 3) mineralization (OC, osteopontin – OP, moderate bALP activity).[6,11,26,27] Cultivation of MSCs in the presence of dex, ascorbic acid, and β-glycerophosphate is the standard procedure for osteogenic differentiation induction under in vitro conditions. Dex, synthetic glucocorticoid, is known to regulate MSC differentiation into osteoblast lineage by activation of intracellular signaling cascades, inter alia

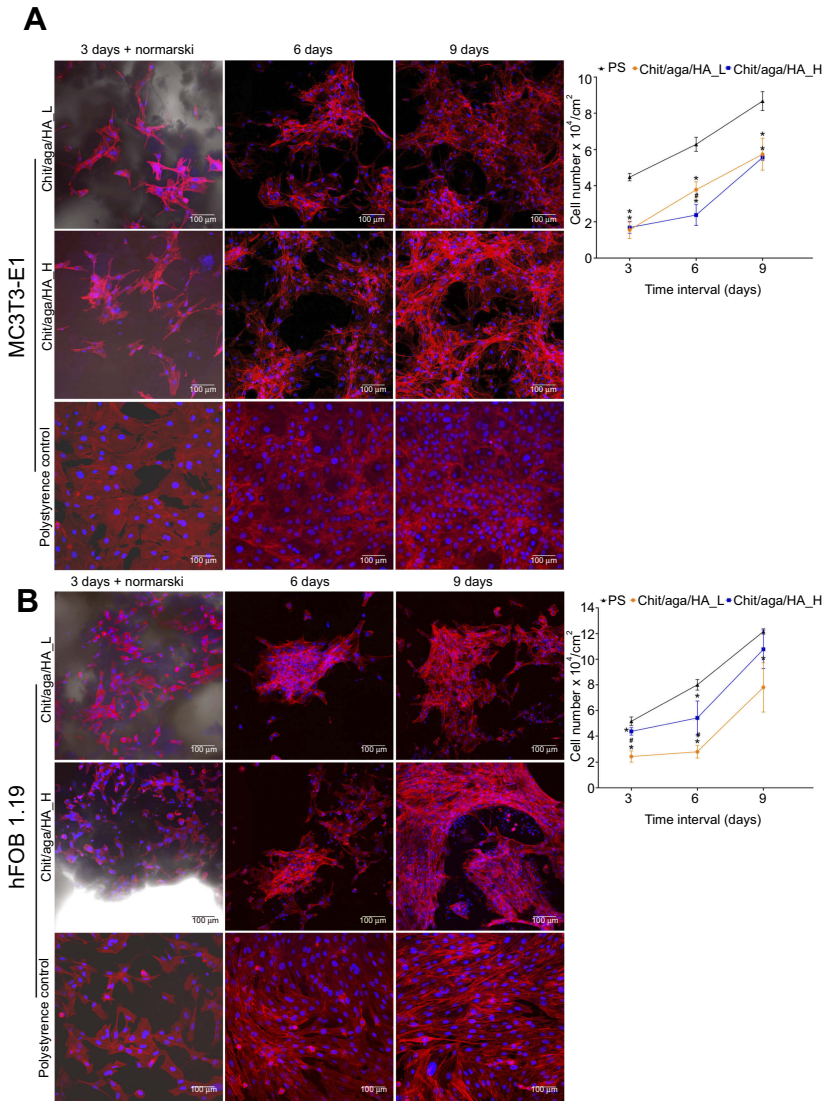

Figure 7 Proliferation of MC3T3-E1 (**A**) and hFOB 1.19 (**B**) osteoblasts on the surface of the bone scaffolds assessed by qualitative analysis via fluorescent staining of cells (cytoskeletal filaments – red fluorescence, nuclei – blue fluorescence; on the 3rd day Nomarski contrast was applied to additionally visualize scaffolds' structure; magnification 200x, scale bar =100 μm) and by quantitative analysis by nuclei counting; polystyrene (PS) – control cells grown in PS well (*statistically significant results compared to PS control in determined time interval; #statistically significant results compared to chit/aga/HA_H in determined time interval, n=3, $P<0.05$, one-way ANOVA followed by Tukey´s test).

Abbreviations: chit/aga/HA_L, chitosan/agarose/nanohydroxyapatite scaffolds with low [40 wt%] nanohydroxyapatite content; chit/aga/HA_H, chitosan/agarose/nanohydroxyapatite scaffolds with high [70 wt%] nanohydroxyapatite content.

WNT/β-catenin signaling pathway, which enhances Runx2 expression.[28,29] In turn, Runx2 – which is an osteoblast-related transcription factor – regulates the expression of genes for bone ECM proteins, such as Col I, OC, OP, and bone sialoprotein.[26] Ascorbic acid is a cofactor for enzymes that hydroxylate proline and lysine during synthesis of collagen and is a predominant regulator of collagen secretion into ECM. Meanwhile, β-glycerophosphate is a phosphate source for the production of HAmineral and it also participates in the regulation of osteogenic gene expression (OP, BMP-2) by extracellular-related kinase phosphorylation.[28,29] Thus, cultivation of MSCs on the novel biomaterials in the osteogenic medium containing ascorbic acid and β-glycerophosphate but without dex, allowed us to determine osteoinductive properties of the scaffolds.

Performed experiments revealed that synthesis of typical osteogenic markers (Runx2, Col I, bALP, OC) by MSCs cultured on the developed nanocomposite scaffolds depends on the source of stem cells (bone marrow or adipose tissue), nanoHA content in the biomaterial (low or high), and the presence/absence of dex in the osteogenic medium. BMDSCs cultured on the chit/aga/HA_L in osteogenic medium without dex (-dex) produced significantly more Col I than cells cultured on the chit/aga/HA_H, whereas ADSCs produced similar amounts of Col I on both scaffolds (Figure 8A). Both

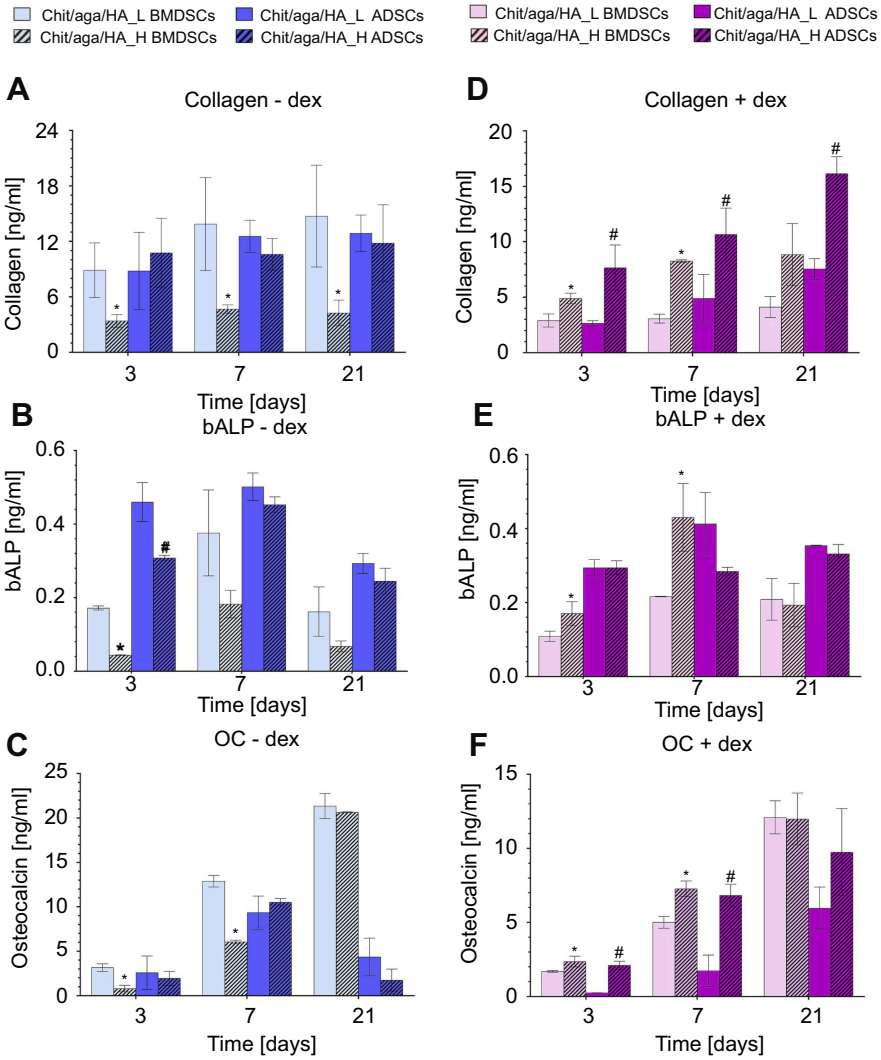

Figure 8 Production of osteogenic differentiation markers (**A**, **D** – collagen, **B**, **E** – bALP, **C**, **F**- OC) by MSCs cultured on the surface of the developed scaffolds and maintained in osteogenic medium without dexamethasone (-dex) (**A**–**C**) and in osteogenic medium with dexamethasone (+dex) (**D**–**F**); *statistically significant results compared to chit/aga/HA_L BMDSCs; #statistically significant results compared to chit/aga/HA_L ADSCs, n=3, $P<0.05$, unpaired *t*-test.

Abbreviations: MSCs, mesenchymal stem cells; BMDSCs, bone marrow-derived mesenchymal stem cells; ADSCs, adipose tissue-derived mesenchymal stem cells; chit/aga/HA_L, chitosan/agarose/nanohydroxyapatite scaffolds with low [40 wt%] nanohydroxyapatite content; chit/aga/HA_H, chitosan/agarose/nanohydroxyapatite scaffolds with high [70 wt%] nanohydroxyapatite content.

types of cells secreted higher amounts of bALP and OC when grown on the chit/aga/HA_L scaffold, however statistically significant results were obtained only on the 3rd day for bALP in ADSCs and BMDSCs and on the 3rd and 7th day for OC in BMDSCs (Figure 8B and C). High synthesis of osteogenic differentiation markers by MSCs cultured in the absence of dex clearly indicated that developed scaffolds had intrinsic osteoinductive properties, proving their excellent biocompatibility. Osteoinductive properties of the biomaterials were also confirmed by IF technique since CLSM images showed not only comparable amounts of Col I on the surface of the biomaterials regardless of the applied medium (+dex or -dex) (Figure 9A and B), but also revealed that on the 7th day, ADSCs cultured on both scaffolds in osteogenic medium/-dex (Figure 10A) showed stronger fluorescence of Runx2 compared to ADSCs cultured in osteogenic medium/+dex (Figure 10B). In the case of BMDSCs, there were no significant differences concerning the strength of fluorescence signal for Runx2 between the cells cultured in osteogenic medium with dex (+dex) and without dex (-dex). It is known that some calcium phosphate-based materials may reveal osteoinductive properties due to their specific topography and microstructure.[8,27,30] However, our studies showed that scaffolds with lower content of bioceramics revealed better osteoinductivity than material containing 70% nanoHA, indicating that induction of osteogenic differentiation in undifferentiated MSCs was induced not only by HA but also by the hybrid chitosan/agarose matrix.

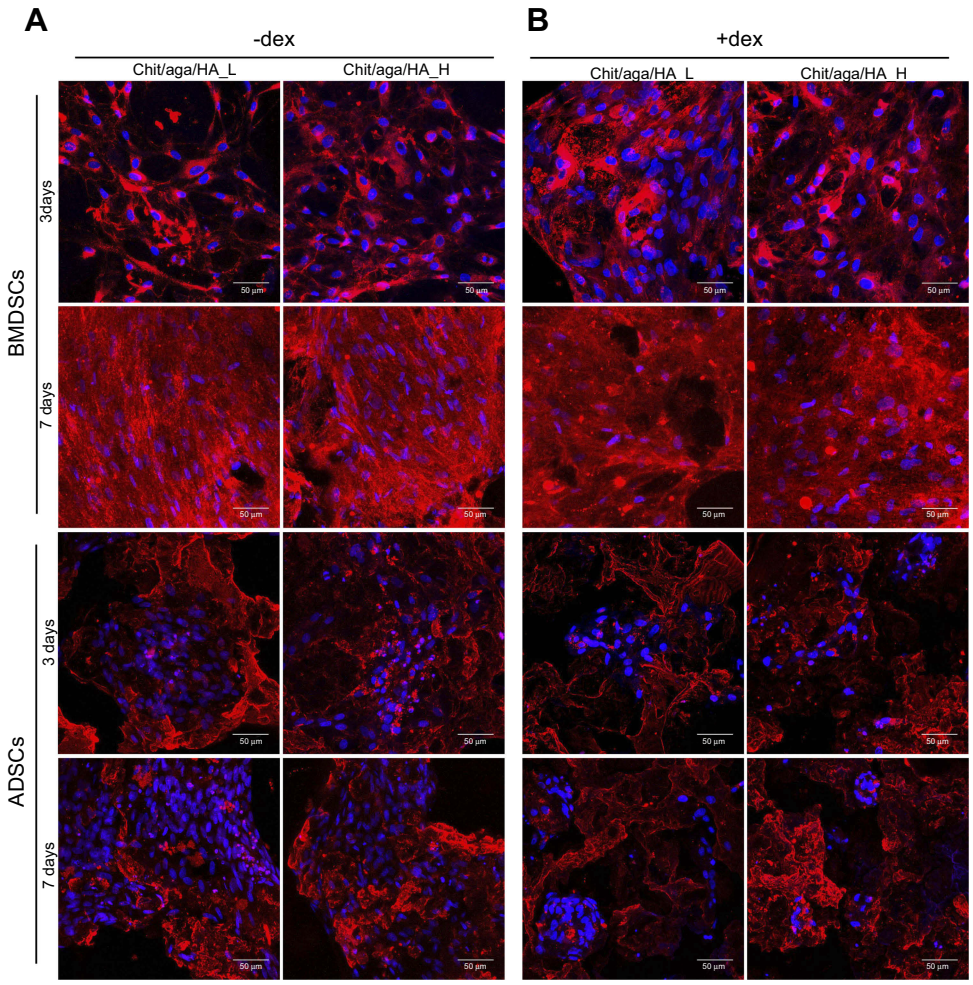

Figure 9 CLSM images showing immunofluorescent staining of type I collagen in the ECM of MSCs cultured on the surface of developed scaffolds and maintained in osteogenic medium without dexamethasone (-dex) (**A**); and in osteogenic medium with dexamethasone (+dex) (**B**); collagen – red fluorescence, nuclei – blue fluorescence, magnification 400x, scale bar =50 µm.

Abbreviations: CLSM, confocal laser scanning microscope; ECM, extracellular matrix; MSCs, mesenchymal stem cells; BMDSCs, bone marrow-derived mesenchymal stem cells; ADSCs, adipose tissue-derived mesenchymal stem cells; chit/aga/HA_L, chitosan/agarose/nanohydroxyapatite scaffolds with low [40 wt%] nanohydroxyapatite content; chit/aga/HA_H, chitosan/agarose/nanohydroxyapatite scaffolds with high [70 wt%] nanohydroxyapatite content.

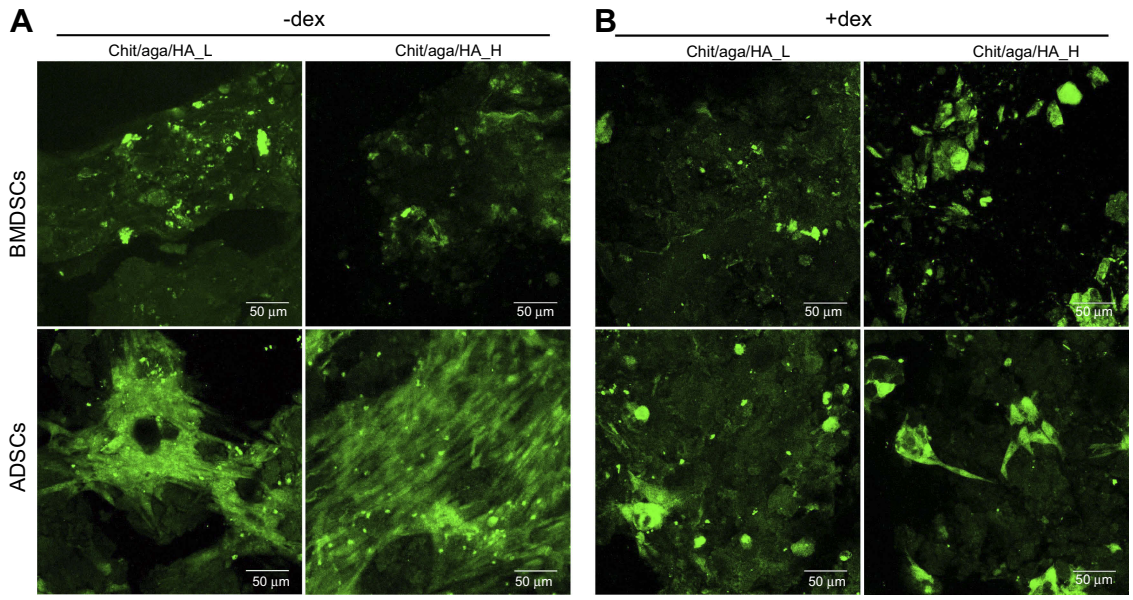

Figure 10 CLSM images showing immunofluorescent staining of Runx2 in the MSCs cultured on the surface of developed scaffolds and maintained in osteogenic medium without dexamethasone (-dex) (**A**) and in osteogenic medium with dexamethasone (+dex) (**B**); Runx2 – green fluorescence, magnification 400x, scale bar =50 µm.
Abbreviations: CLSM, confocal laser scanning microscope; ECM, extracellular matrix; MSCs, mesenchymal stem cells; BMDSCs, bone marrow-derived mesenchymal stem cells; ADSCs, adipose tissue-derived mesenchymal stem cells; chit/aga/HA_L, chitosan/agarose/nanohydroxyapatite scaffolds with low [40 wt%] nanohydroxyapatite content; chit/aga/HA_H, chitosan/agarose/nanohydroxyapatite scaffolds with high [70 wt%] nanohydroxyapatite content.

Interestingly, the results obtained with the use of osteogenic medium with dex (+dex) were completely different. BMDSCs cultured on the chit/aga/HA_H produced significantly higher amounts of Col I, bALP, and OC on the 3rd and 7th day of the experiment than those cultured on the chit/aga/HA_L (Figure 8D–F). ADSCs followed this trend for the Col I and OC (Figure 8D and F). Experiments performed with the use of osteogenic medium/+dex clearly demonstrated that both developed scaffolds were biocompatible and allowed for MSC-mediated bone formation on their surfaces. CLSM images presenting great deposits of Col I protein on the surface of biomaterials confirmed their high biocompatibility (Figure 9B). Interestingly, a higher content of nanoHA in the scaffold significantly improved its osteoconductivity, which is in good agreement with the data found in the available literature, showing great osteoconductive properties of HA and improvement of biocompatibility of implants after their modifications with calcium-phosphate bioceramics.[8,31,32]

Interestingly, it was also observed that ADSCs generally synthesized higher amounts of Col I and bALP, but lower OC compared to BMDSCs regardless of the type of osteogenic medium used (+dex or -dex) (Figure 8A–F). Since bALP is an enzyme with the highest activity during ECM synthesis, and OC is a late osteogenic differentiation marker involved in ECM mineralization,[6,11,26,27] it may be suggested that ADSCs cultured on the developed scaffolds had superior ability to produce ECM proteins and inferior mineralization capability compared to BMDSCs. Similar results were obtained in our other studies, where ADSCs showed a noticeably lower ability to produce OC compared to BMDSCs during their culture on the surface of chitosan/β-1,3-glucan/HA scaffold.[33]

Conclusion

Obtained results clearly showed that both fabricated by novel method nanocomposite scaffolds were characterized by high biocompatibility, osteoconductive, and osteoinductive properties. The surface of novel biomaterials is extremely hydrophilic, prone to protein adsorption with the highest affinity toward fibronectin binding, which allows for good osteoblast adhesion, spreading, and proliferation. Investigated biomaterials exhibit similar biocompatibility regardless of bioceramic content, however, the scaffold with a lower content of nanoHA revealed significantly better osteoinductive properties. Furthermore, chit/aga/HA_L has a different surface chemical composition (most notably, higher share of OH group, presence of protonated amide), which slightly reduces its protein adsorption ability compared to the scaffold with higher content of nanoHA. By studying cellular responses to the surface of chitosan/agarose/nanoHA scaffolds, we proved that applied novel

fabrication method allowed us to obtain macroporous biomaterials with great potential to be used in BTE to support and accelerate bone regeneration.

Acknowledgments

Financial support was provided by National Science Centre (NCN) (Poland) with OPUS 16 grant number UMO-2018/31/B/ST8/00945. Analysis performed by Aleksandra Benko was supported by the NCN in Poland with grant number UMO-2017/24/C/ST8/00400. This paper was developed using the equipment purchased within agreement number POPW.01.03.00-06-010/09-00 Operational Program Development of Eastern Poland 2007–2013, Priority Axis I, Modern Economy, Operations 1.3. Innovations Promotion.

Disclosure

Paulina Kazimierczak and Agata Przekora report grants from NCN and Operational Program Development of Eastern Poland 2007–2013, during the conduct of the study; in addition, they have a patent, PL number P.426788, pending. Aleksandra Benko reports a grant from NCN, outside the submitted work. The authors report no other conflicts of interest in this work.

References

1. Madhumathi K, Shalumon KT, Rani VVD, et al. Wet chemical synthesis of chitosan hydrogel – hydroxyapatite composite membranes for tissue engineering applications. *Int J Biol Macromol*. 2009;45:12–15. doi:10.1016/j.ijbiomac.2009.03.011
2. Muzzarelli RAA. Chitosan composites with inorganics, morphogenetic proteins and stem cells, for bone regeneration. *Carbohydr Polym*. 2011;83:1433–1445. doi:10.1016/j.carbpol.2010.10.044
3. Zarrintaj P, Manouchehri S, Ahmadi Z, et al. Agarose-based biomaterials for tissue engineering. *Carbohydr Polym*. 2018;187:66–84. doi:10.1016/j.carbpol.2018.01.060
4. Felfel RM, Gideon-adeniyi MJ, Zakir KM, Roberts GAF, Grant DM. Structural, mechanical and swelling characteristics of 3D scaffolds from chitosan-agarose blends. *Carbohydr Polym*. 2019;204:59–67. doi:10.1016/j.carbpol.2018.10.002
5. Morais JM, Papadimitrakopoulos F, Burgess DJ. Biomaterials/tissue interactions: possible solutions to overcome foreign body response. *Am Assoc Pharm Sci*. 2010;12(2):188–196. doi:10.1208/s12248-010-9175-3
6. Przekora A. The summary of the most important cell-biomaterial interactions that need to be considered during in vitro biocompatibility testing of bone scaffolds for tissue engineering applications. *Mater Sci Eng C*. 2019;97:1036–1051. doi:10.1016/J.MSEC.2019.01.061
7. Stevens MM. Biomaterials for bone tissue engineering. *Mater Today*. 2008;11(5):18–25. doi:10.1016/S1369-7021(08)70086-5
8. Xu HH, Wang P, Wang L, et al. Calcium phosphate cements for bone engineering and their biological properties. *Bone Res*. 2017;5:17056. doi:10.1038/boneres.2017.56
9. Duan G, Greiner A. Air-blowing-assisted coaxial electrospinning toward high productivity of core/sheath and hollow fibers. *Macromol Mater Eng*. 2019;304(5):2–6. doi:10.1002/mame.201800669
10. Przekora A, Ginalska G. In vitro evaluation of the risk of inflammatory response after chitosan/HA and chitosan/β-1,3-glucan/HA bone scaffold implantation. *Mater Sci Eng C*. 2016;61. doi:10.1016/j.msec.2015.12.066
11. Przekora A, Ginalska G. Enhanced differentiation of osteoblastic cells on novel chitosan/β-1,3-glucan/bioceramic scaffolds for bone tissue regeneration. *Biomed Mater*. 2015;10:1. doi:10.1088/1748-6041/10/1/015009
12. Estes BT, Diekman BO, Gimble JM, Guilak F. Isolation of adipose derived stem cells and their induction to a chondrogenic phenotype. *Nat Protoc*. 2010;5(7):1294–1311. doi:10.1038/nprot.2010.81
13. López-Pérez PM, Da Silva RMP, Serra C, Pashkuleva I, Reis RL. Surface phosphorylation of chitosan significantly improves osteoblast cell viability, attachment and proliferation. *J Mater Chem*. 2010;20:483–491. doi:10.1039/b911854c
14. Maachou H, Genet MJ, Aliouche D, Dupont-Gillain CC, Rouxhet PG. XPS analysis of chitosan-hydroxyapatite biomaterials: from elements to compounds. *Surf Interface Anal*. 2013;45(7):1088–1097. doi:10.1002/sia.5229
15. Rabe M, Verdes D, Seeger S. Understanding protein adsorption phenomena at solid surfaces. *Adv Colloid Interface Sci*. 2011;162(1–2):87–106. doi:10.1016/j.cis.2010.12.007
16. Chang H-I, Wang Y. Cell responses to surface and architecture of tissue engineering scaffolds. In: Eberli D, editor. *Regenerative Medicine and Tissue Engineering - Cells and Biomaterials*. Croatia: InTech; 2011:569–588. doi:10.5772/21983
17. Brevig T, Holst B, Ademovic Z, et al. The recognition of adsorbed and denatured proteins of different topographies by β2 integrins and effects on leukocyte adhesion and activation. *Biomaterials*. 2005;26(16):3039–3053. doi:10.1016/j.biomaterials.2004.09.006
18. Santos SG, Lamghari M, Almeida CR, et al. Adsorbed fibrinogen leads to improved bone regeneration and correlates with differences in the systemic immune response. *Acta Biomater*. 2013;9(7):7209–7217. doi:10.1016/j.actbio.2013.04.008
19. Maciel J, Oliveira MI, Colton E, et al. Adsorbed fibrinogen enhances production of bone- and angiogenic-related factors by monocytes/macrophages. *Tissue Eng Part A*. 2014;20(1–2):250–263. doi:10.1089/ten.tea.2012.0439
20. Li S, Yu W, Zhang W, Zhang G, Yu L, Lu E. Evaluation of highly carbonated hydroxyapatite bioceramic implant coatings with hierarchical micro-/nanorod topography optimized for osseointegration. *Int J Nanomedicine*. 2018;13:3643–3659. doi:10.2147/IJN.S159989
21. Keselowsky BG, Collard DM, García AJ. Surface chemistry modulates fibronectin conformation and directs integrin binding and specificity to control cell adhesion. *J Biomed Mater Res Part A*. 2003;66(2):247–259. doi:10.1002/jbm.a.10537
22. Lee MH, Ducheyne P, Lynch L, Boettiger D, Composto RJ. Effect of biomaterial surface properties on fibronectin– α5β1 integrin interaction and cellular attachment. *Biomaterials*. 2006;27:1907–1916. doi:10.1016/j.biomaterials.2005.11.003
23. Mosesson MW. Structure and functions of fibrinogen and fibrin. In: Tanaka K, Davie EW, Ikeda Y, Iwanaga S, Saito H, Sueishi K, editors. *Recent Advances in Thrombosis and Hemostasis 2008*. Tokyo: Springer; 2008:3–26. doi:10.1007/978-4-431-78847-8_1
24. Schneider GB, English A, Abraham M, Zaharias R, Stanford C, Keller J. The effect of hydrogel charge density on cell attachment. *Biomaterials*. 2004;25(15):3023–3028. doi:10.1016/j.biomaterials.2003.09.084
25. Sachot N, Engel E, Castano O. Hybrid organic-inorganic scaffolding biomaterials for regenerative therapies. *Curr Org Chem*. 2014;18(18):2299–2314. doi:10.2174/1385272819666140806200355
26. Neve A, Corrado A, Cantatore FP. Osteoblast physiology in normal and pathological conditions. *Cell Tissue Res*. 2011;343:289–302. doi:10.1007/s00441-010-1086-1

27. Tang Z, Li X, Tan Y, Fan H, Zhang X. The material and biological characteristics of osteoinductive calcium phosphate ceramics. *Regen Biomater*. 2018;5(1):43–59. doi:10.1093/rb/rbx024
28. Langenbach F, Handschel J. Effects of dexamethasone, ascorbic acid and β-glycerophosphate on the osteogenic differentiation of stem cells in vitro. *Stem Cell Res Ther*. 2013;4(5):117. doi:10.1186/scrt328
29. Freeman FE, Stevens HY, Owens P, Guldberg RE, McNamara LM. Osteogenic differentiation of mesenchymal stem cells by mimicking the cellular niche of the endochondral template. *Tissue Eng Part A*. 2016;22(19–20):1176–1190. doi:10.1089/ten.tea.2015.0339
30. Legeros RZ. Calcium phosphate-based osteoinductive materials. *Chem Rev*. 2008;108:4742–4753. doi:10.1021/cr800427g
31. Swetha M, Sahithi K, Moorthi A, Srinivasan N, Ramasamy K, Selvamurugan N. Biocomposites containing natural polymers and hydroxyapatite for bone tissue engineering. *Int J Biol Macromol*. 2010;47(1):1–4. doi:10.1016/j.ijbiomac.2010.03.015
32. Kuroda K, Okido M. Hydroxyapatite coating of titanium implants using hydroprocessing and evaluation of their osteoconductivity. *Bioinorg Chem Appl*. 2012;2012:730693. doi:10.1155/2012/730693
33. Przekora A, Vandrovcova M, Travnickova M, et al. Evaluation of the potential of chitosan/β-1,3-glucan/hydroxyapatite material as a scaffold for living bone graft production in vitro by comparison of ADSC and BMDSC behaviour on its surface. *Biomed Mater*. 2017;12:1. doi:10.1088/1748-605X/aa56f9